MINERALOGICAL MAGAZINE, DECEMBER 1986, VOL. 50, PP. 597–610

The mineralogy of nepheline syenite complexes from the northern part of the Chilwa Province, Malawi

ALAN R. WOOLLEY

Department of Mineralogy, British Museum (Natural History), Cromwell Road, London SW7 5BD, UK

AND

R. GARTH PLATT

Department of Geology, Lakehead University, Thunder Bay, Ontario, Canada

ABSTRACT. The mineralogy, including the accessory phases låvenite, rosenbuschite, and catapleiite, and consequent petrogenetic implications have been investigated for a group of four overlapping nepheline syenite complexes (Chikala, Chaone, Mongolowe, and Chinduzi) and for spatially associated silica-saturated and oversaturated perthosites, from the northern part of the Chilwa Alkaline Province, Malawi.

The complexes are thought to have formed by injection into high-level chambers of magma pulses genetically related to a common source magma at depth. Evidence for the source magma is preserved in salitic cores observed in the pyroxenes and a trend to more hedenbergite-rich compositions is believed to have formed by evolution of this magma. Subsequent trends of acmite enrichment followed magma injection into the higher-level chambers; the actual pyroxene trend associated with each individual complex is a function of the evolution attained by the source magma, oxidation potential, and perhaps even alkali activity. On the basis of such a two-stage model, the pyroxene data suggest emplacement of the Chaone and Mongolowe magmas somewhat earlier than that of Chikala, with the Chinduzi magma migrating even later.

Amphiboles and biotites are believed to have formed after high-level injection of the magmas. Their compositions broadly reflect the nature of the crystallizing pyroxenes in that magnesian hastingsitic hornblendes and more Mg-rich biotites are associated with more Mg-rich sodic pyroxenes, whereas katophorites and annite-rich micas are generally associated with sodic pyroxenes somewhat richer in hedenbergite. Sub-solidus crystallization in some of the complexes is represented by aegirine and magnesio-arfvedsonite. Nepheline compositions indicate broadly similar crystallization temperatures within the complexes, namely 950 to 750 °C. Oxygen fugacities for these magmas obtained from biotite/annite compositions vary from 10^{-19} to 10^{-14} bars for this temperature range. Mineralogical data, particularly from pyroxenes and amphiboles, strongly suggest that the perthosites, spatially associated with the nepheline syenite complexes, are genetically unrelated.

KEYWORDS: nepheline syenite, pyroxene, amphibole, mica, låvenite, rosenbuschite, catapleiite, Chilwa, Malawi.

THE Chilwa Alkaline Province, situated at the southern end of the East African Rift system, is dominated by intrusive rocks falling broadly into three categories. In order of volumetric abundance these are: (1) Granites and silica-saturated to oversaturated syenites which are often peralkaline in nature, e.g. Mulanje (Platt and Woolley, 1986) and Zomba (Bloomfield, 1965); (2) Nepheline syenites and silica-saturated syenites, studies of which form the basis of this paper; (3) Carbonatites and related minor intrusions of nephelinite and nepheline syenite represented in part by the classic localities of Chilwa Island (Garson and Smith, 1958) and Tundulu (Garson, 1962).

Earlier work on the Province was mainly directed towards field and petrographic descriptions. Until recently (e.g. Platt and Woolley, 1986; Woolley and Jones, in press), detailed studies of geochemistry and mineralogy had not been undertaken.

This paper investigates principally the mineralogy and petrogenetic implications of a group of four overlapping nepheline syenite complexes lying some 20 km north of Zomba (fig. 1). These complexes of Chikala, Chaone, Mongolowe and Chinduzi are the largest centres of nepheline syenite–syenite magmatism in the northern part of the Chilwa Province. Earlier work by Garson (1960) and Stillman and Cox (1960) on Chikala, by Vail and Monkman (1960) on Chaone, by Vail and Mallick (1965) on Mongolowe, and by Bloomfield (1965) on Chinduzi, indicate that each body has a complex pattern of intrusions which often take

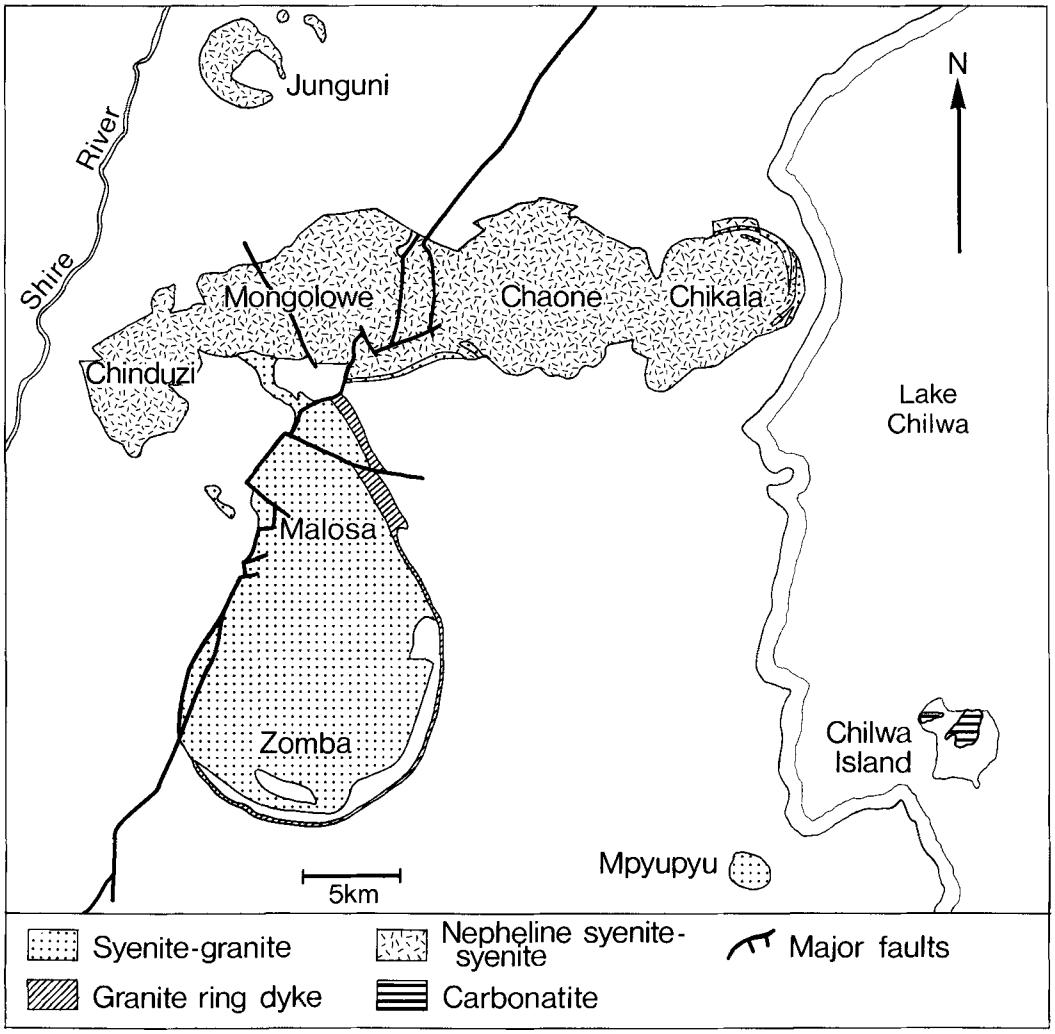

FIG. 1. The major intrusions of the northern part of the Chilwa Alkaline Province, Malawi.

annular form. The field relationships seem to indicate an increase in the age of the complexes from east to west but the scarcity of age data make this difficult to confirm (Woolley and Garson, 1970, Table 1).

The predominant rock types were mapped as pulaskite and foyaite, but when the four complexes are considered together, a continuum of compositions is seen to extend from the feldspar to phonolite minima in the system nepheline-kalsilite-silica (Woolley and Jones, in press). These same authors also point out an increasing silica-undersaturation and peralkalinity of the complexes from east to west (fig. 1). The most silica-undersaturated and peralkaline intrusion in the region, Junguni, lies just to the north of Mongolowe (fig. 1) and is the subject of a forthcoming paper by Woolley and Platt.

Narrow strips and arcuate intrusions of silica-saturated to silica-oversaturated syenites are found within Chikala and Chaone and the mafic mineralogy of these syenites, as will be shown in this paper, suggests that their origin is unrelated to the formation of the nepheline syenites. This is also apparent from their geochemistry (Woolley and Jones, in press), and these authors postulate a consanguinity with the syenites and peralkaline granites of the nearby Zomba pluton.

The presence of xenoliths and small down-faulted masses of nephelinitic volcanic rocks in the complexes (Woolley and Jones, in press), and the interpretation of the emplacement of some of the complexes by cauldron subsidence (Bloomfield, 1965), indicate a relatively shallow level of emplacement.

Petrography

Earlier workers on the four centres of Chikala, Chaone, Mongolowe, and Chinduzi mapped and described the nepheline syenites as pulaskites, foyaites, and microfoyaites. The minor silica-saturated to oversaturated syenites were termed by them perthosite. Although there were slight differences in the definitions adopted, pulaskites were generally defined as rocks with up to 5% modal nepheline and 5 to 50% modal mafic minerals. Foyaites contained between 5 and 50% modal nepheline whereas perthosites were defined as alkali feldspar-rich rocks with up to 5% modal quartz.

The pulaskites and foyaites vary from coarse-grained rocks with feldspar plates and patches of mafic minerals over 1 cm in diameter, to finer-grained more homogeneous varieties. Alkali feldspar shows a wide range of complex exsolution and replacement textures. Nepheline is usually fresh and occurs as subhedral prisms, intersertal patches or as numerous rounded and optically continuous blebs within the feldspar. Sodalite, occurring interstitially or as a replacement of both feldspar and nepheline, is found in many of the foyaites and in the most peralkaline of the four complexes, Chinduzi; it may constitute as much as 20% by volume of some rocks.

Pyroxenes with pale green–brown cores, generally surrounded by pleochroic green rims, are relatively common in rocks from Mongolowe and Chaone. The pale cores are less common in Chikala and only occasionally seen in the pyroxenes of Chaone; in the latter, green pleochroic pyroxenes predominate. Late-stage, subsolidus deep green sodic pyroxenes, generally associated with patches or narrow veins of blue-green to blue sodic amphiboles were noted in a few rocks, particularly from Mongolowe and Chaone. Pyroxenes are commonly replaced by amphibole, with this phenomenon more apparent in rocks of Chikala, Mongolowe, and Chaone. In addition to replacing pyroxene, the amphiboles may also occur as euhedral prisms, spongy poikilitic crystals or in patches with biotite, pyroxene, sphene, apatite, and an opaque oxide phase.

Biotite is present in most rocks and in many pulaskites it is particularly abundant, forming crystals up to 0.5 cm in diameter. An opaque oxide phase, now invariably magnetite with exsolved ilmenite, is common in most rocks. Accessory phases include apatite, sphene, and zircon. Rosenbuschite, låvenite, catapleiite, and sphalerite have been identified in rocks from Chinduzi, as have låvenite and zirconolite in Chikala nepheline syenite.

The perthosites are generally coarse-grained with large plates of perthite, subhedral amphibole, often with cores of pyroxene, and minor biotite. Modal quartz is present in three of the perthosites investigated. Apatite, zircon, sphene, and an opaque phase are ubiquitous accessory minerals. Fayalite and chevkinite have also been identified.

Mineralogy

A selection of thirty-three samples, covering all the important rock types of the four complexes, were chosen for detailed mineralogical studies by electron microprobe. Particular emphasis was placed on characterizing the nature and trends observed in nephelines, pyroxenes, amphiboles, and micas. The microprobe studies were performed at the British Museum (Natural History) using a Cambridge Instruments Geoscan and

TABLE I.

REPRESENTATIVE ANALYSES OF NEPHELINE

	1	2	3	4	5
SiO_2	45.74	44.61	44.86	45.20	44.36
Al_2O_3	32.50	32.77	32.22	32.55	32.16
Fe_2O_3*	0.39	0.42	0.72	0.69	0.80
CaO	0.19	0.17	0.07	0.24	0.07
Na_2O	15.65	15.99	15.61	16.26	15.66
K_2O	5.14	5.88	5.93	4.98	5.97
Total	99.61	99.84	99.41	99.92	99.02
Structural formula calculated on the basis of 32 oxygens					
Si	8.710	8.545	8.622	8.613	8.575
Al	7.295	7.398	7.299	7.311	7.327
Fe^{3+}	0.056	0.061	0.104	0.099	0.116
Ca	0.039	0.035	0.014	0.049	0.014
Na	5.779	5.938	5.817	6.008	5.869
K	1.249	1.437	1.454	1.211	1.472
Weight per cent end-member molecules					
Ne	73.44	74.00	72.40	75.70	72.81
Ks	17.84	20.14	20.52	17.27	20.75
Qz	8.72	5.86	7.08	7.03	6.45

Fe_2O_3* total iron calculated as Fe_2O_3

Ne = $NaAlSiO_4$; Ks = $KAlSiO_4$; Qz = SiO_2

1-2 Mongolowe; 3 Chaone; 4 Chikala; 5 Chinduzi

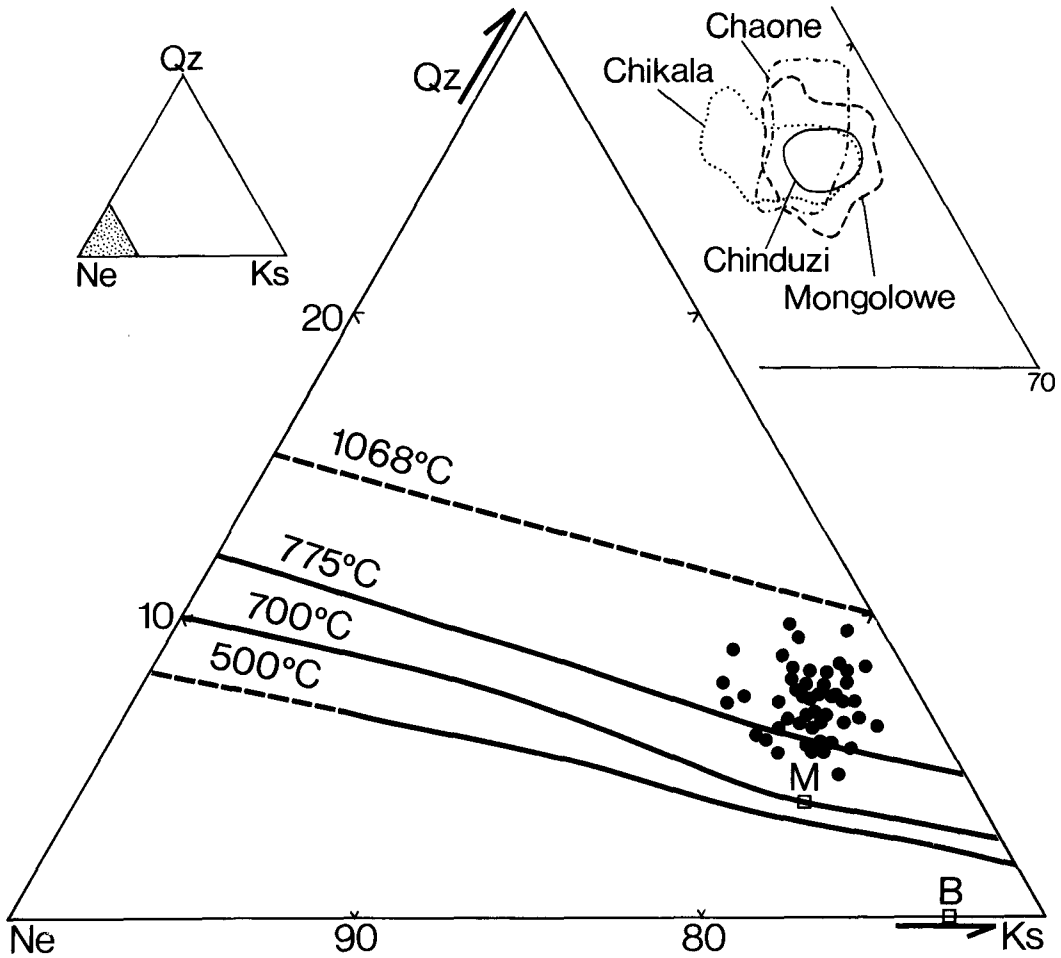

FIG. 2. Nepheline compositions plotted in a portion of the system nepheline–kalsilite–silica (wt. %). The isotherms show the limits of nepheline solid solution at the indicated temperatures (after Hamilton, 1961). M and B are Morozewicz and Buerger ideal nepheline compositions. The inset diagram shows the areas occupied by analyses for each of the four nepheline syenite complexes.

Link Systems energy dispersive analyser. Live time counts of 100 seconds and an acceleration voltage of 15 kV were the general conditions of analysis.

Nepheline. Compositional variations of nepheline from the various complexes are shown together in fig. 2; typical analyses are given in Table I. Taken as a group, the nepheline compositions show minor compositional variations and in terms of the end-member components nepheline–kalsilite–silica, nephelines from each complex overlap compositionally (fig. 2, inset). The excess of Si over that required by stoichiometry indicates crystallization temperatures in the general range of 750 to 950 °C (Hamilton, 1961). This is significantly higher than typical plutonic nephelines which generally lie within the Morozewicz–Buerger convergence field (Tilley, 1954) (fig. 2). The importance of this will be discussed later in the paper, but rather rapid cooling, as perhaps found in sub-volcanic magma chambers, would be required to retain the 'high'-temperature nepheline compositions.

Pyroxene. Representative analyses of pyroxenes from the nepheline syenites and perthosites are given in Tables II and III, respectively. Compositional variations, in terms of acmite, diopside, and hedenbergite, for the pyroxenes of each individual complex and the perthosites are shown in fig. 3*a–d*

TABLE II

REPRESENTATIVE ANALYSES OF PYROXENES FROM THE NEPHELINE SYENITES

	1	2	3	4	5	6	7	8	9	10	11	12
SiO_2	49.60	51.71	49.21	50.17	49.79	50.54	51.12	51.05	49.02	49.75	49.61	50.53
TiO_2	0.98	0.26	0.79	0.40	0.25	0.56	0.43	0.73	0.69	0.99	0.51	0.44
Al_2O_3	3.04	0.75	2.17	1.07	5.26	1.46	1.54	0.32	1.00	0.90	1.06	1.04
Fe_2O_3*	6.05	3.99	4.36	3.87	12.84	15.96	12.11	16.92	10.65	14.40	11.03	27.12
FeO	5.33	9.76	11.58	13.99	4.05	7.25	6.56	7.03	13.09	10.37	12.39	3.08
MnO	0.63	0.83	1.09	1.21	0.94	1.28	1.13	1.69	1.22	1.24	1.05	0.65
MgO	10.45	9.54	7.05	7.29	5.94	3.46	6.55	3.25	2.77	2.19	3.46	0.48
CaO	21.40	22.00	20.77	20.61	16.73	11.83	16.57	12.19	15.36	13.67	15.44	5.54
Na_2O	1.85	1.41	1.73	1.27	4.93	6.85	4.53	6.92	4.52	5.98	4.46	10.60
ZrO_2	0.68	0.45	0.56	0.26	0.21	1.20	0.17	0.93	1.14	0.67	0.52	0.25
Total	100.01	100.70	99.31	100.14	100.94	100.39	100.71	101.08	99.46	100.16	99.53	99.73
Structural formula based on 4 cations and 6 oxygens												
Si	1.874	1.962	1.918	1.950	1.871	1.953	1.944	1.967	1.949	1.952	1.957	1.961
Al	0.135	0.034	0.100	0.049	0.233	0.066	0.069	0.015	0.047	0.042	0.049	0.048
Ti	0.028	0.007	0.023	0.012	0.007	0.016	0.012	0.021	0.021	0.029	0.015	0.013
Fe^{3+}*	0.172	0.114	0.128	0.113	0.363	0.464	0.347	0.491	0.319	0.425	0.328	0.794
Fe^{2+}	0.168	0.310	0.377	0.455	0.127	0.234	0.209	0.227	0.435	0.340	0.409	0.100
Mn	0.020	0.027	0.036	0.040	0.030	0.042	0.036	0.055	0.041	0.041	0.035	0.021
Mg	0.588	0.540	0.409	0.422	0.333	0.199	0.371	0.187	0.164	0.128	0.203	0.028
Ca	0.866	0.895	0.867	0.858	0.674	0.490	0.675	0.503	0.654	0.575	0.653	0.231
Na	0.136	0.104	0.131	0.096	0.359	0.513	0.334	0.517	0.348	0.455	0.341	0.799
Zr	0.013	0.008	0.011	0.005	0.004	0.023	0.003	0.017	0.022	0.013	0.010	0.005
Molecular per cent of end-member molecules												
Di	65.14	55.05	43.05	41.27	44.63	21.21	39.60	20.23	17.27	13.89	20.73	2.95
Hd	20.87	34.33	43.45	48.34	21.09	29.41	26.13	30.54	50.12	41.36	45.23	12.88
Ac	13.99	10.62	13.50	10.39	34.28	49.38	34.27	49.24	32.61	44.75	34.05	84.17

Fe_2O_3* calculated on the basis of 4 cations and 6 oxygens

Di = $CaMgSi_2O_6$; Hd = $CaFe^{2+}Si_2O_6$; Ac = $NaFe^{3+}Si_2O_6$. Proportions calculated after the method of Larsen (1976).

1-4 representative of the Salite Trend; 5-6 Mongolowe sodic pyroxenes; 7-8 Chaone sodic pyroxenes; 9-10 Chikala sodic pyroxenes; 11-12 Chinduzi sodic pyroxenes.

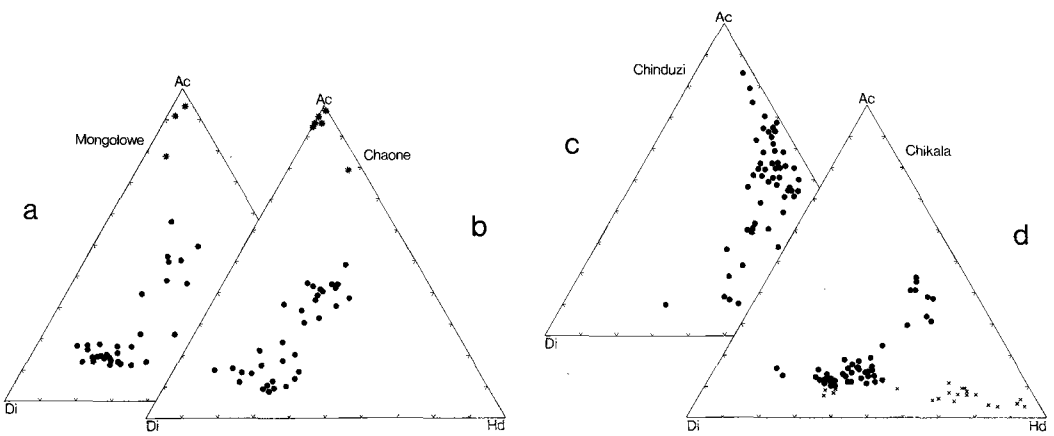

FIG. 3*a–d*. Compositional variations of pyroxenes plotted in terms of acmite–diopside–hedenbergite. The star symbols on *a* and *b* are for sub-solidus aegirines; crosses on *d* represent pyroxenes from perthosites.

and the trends of pyroxene evolution, in terms of the same end-member pyroxene components, are shown in fig. 4.

TABLE III

REPRESENTATIVE ANALYSES OF PYROXENES FROM QUARTZ SYENITES

	1	2	3	4
SiO_2	50.91	49.40	49.45	47.16
TiO_2	0.25	0.15	0.09	0.50
Al_2O_3	0.65	1.02	0.29	0.56
Fe_2O_3*	3.94	4.42	2.42	3.33
FeO	10.59	16.07	21.27	26.66
MnO	1.09	1.31	1.53	1.14
MgO	10.83	6.56	3.67	0.73
CaO	19.67	19.71	20.43	19.77
Na_2O	1.08	1.07	0.92	0.54
ZrO_2	0.17	0.16	0.13	0.19
Total	99.18	99.87	100.20	100.58
Structural formula based on 4 cations and 6 oxygens				
Si	1.958	1.944	1.987	1.937
Al	0.029	0.047	0.014	0.027
Ti	0.007	0.004	0.003	0.015
Fe^{3+}*	0.114	0.131	0.073	0.103
Fe^{2+}	0.340	0.529	0.715	0.916
Mn	0.036	0.044	0.052	0.040
Mg	0.621	0.385	0.220	0.045
Ca	0.811	0.831	0.862	0.870
Na	0.081	0.082	0.072	0.043
Zr	0.003	0.003	0.003	0.004
Moleculer per cent of end-member molecules				
Di	56.44	36.40	20.57	4.31
Hd	34.19	54.16	71.79	92.15
Ac	9.37	9.44	7.64	3.54

Fe_2O_3* calculated on the basis of 4 cations and 6 oxygens

Di=$CaMgSi_2O_6$; Hd=$CaFe^{3+}Si_2O_6$;

Ac=$NaFe^{3+}Si_2O_6$;

proportions calculated after the method of Larsen (1976).

Commonly, the sodian salites in each of the complexes occur as pale green–brown cores which in turn are overgrown by green aegirine–augite. Salitic cores are more common in pyroxenes from Chaone and Mongolowe than in those from Chikala, but are scarce in Chinduzi rocks. The salites from the four complexes as a whole show a general evolution towards hedenbergite with between 10 and 20 mol. % acmite (fig. 4). In the discussion which follows, this will be referred to as the salitic trend.

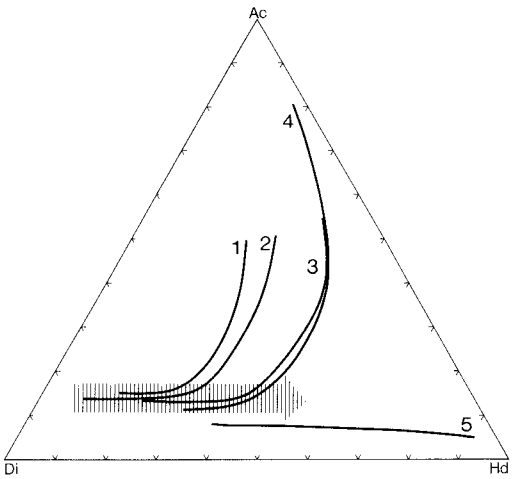

FIG. 4. General pyroxene trends in terms of acmite–diopside–hedenbergite. (1) Mongolowe; (2) Chaone; (3) Chikala; (4) Chinduzi; (5) Perthosites. The broad arrow represents the 'salitic trend'—for explanation see text.

In general terms, the pyroxenes of the nepheline syenite complexes become enriched in acmite with individual trends originating from sodian-salitic compositions (fig. 4). The trends of Mongolowe and Chaone originate from diopside-rich salites and terminate with relatively Mg-rich aegirine–augites. Within these complexes, subsolidus metasomatic aegirine is occasionally observed in association with magnesio-arfvedsonite (figs 3*a* and *b*). The aegirine–augites of Chikala are considerably richer in hedenbergite than those of Chaone and Mongolowe (fig. 3*d*) and the earlier salitic pyroxenes tend also to be richer in hedenbergite (fig. 3*d*). The most extreme sodium-enrichment in pyroxene compositions is found in rocks from Chinduzi in which the compositional trend terminates with aegirine (fig. 3*c*). Salitic pyroxenes are rather scarce but where seen, as remnant cores, they tend to be relatively enriched in hedenbergite (fig. 3*c*).

Salites in the perthosites (fig. 3*d*) are substantially different from those in the nepheline syenites. They evolve to compositions rich in hedenbergite and contain significantly less acmite (fig. 4). Petrogenetically, they appear unrelated to the pyroxenes of the nepheline syenites. They show, in fact, greater similarities with pyroxenes associated with the peralkaline granites and quartz syenites of Mulanje (Platt and Woolley, 1986). Petrographically it seems as though the silica-oversaturated perthosites are unrelated to the nepheline syenites.

TABLE IV

REPRESENTATIVE ANALYSES OF AMPHIBOLES

	1	2	3	4	5	6	7	8
SiO_2	38.74	40.69	42.94	42.31	47.68	49.95	50.62	43.93
Al_2O_3	10.21	9.36	7.83	6.45	3.76	2.25	1.81	4.79
TiO_2	1.26	2.00	1.63	2.10	1.23	1.08	0.67	0.94
Fe_2O_3*	6.94	2.57	3.42	4.74	2.92	1.94	7.83	6.50
FeO	20.61	19.54	17.09	23.91	18.75	16.29	14.68	21.97
MnO	0.97	1.28	1.30	1.35	1.25	1.25	0.92	1.54
MgO	4.40	7.06	8.62	3.34	8.45	11.21	9.39	4.77
CaO	8.89	9.53	8.72	6.16	5.87	6.37	2.20	9.79
Na_2O	3.80	4.06	4.45	5.43	5.95	6.10	7.77	1.95
K_2O	1.87	1.71	1.57	1.63	1.66	1.22	1.99	1.17
ZrO_2	0.16	0.10	0.41	0.55	0.14	0.15	0.07	0.13
Total	97.85	97.90	97.98	97.97	97.66	97.81	97.95	97.48
Structural formula based on 13 cations and 23 oxygens								
Si	6.169	6.361	6.614	6.754	7.323	7.522	7.631	6.962
Al^{IV}	1.831	1.639	1.386	1.214	0.677	0.399	0.322	0.895
Fe^{3+IV}	-	-	-	0.032	-	0.079	0.047	0.143
Σ	8.000	8.000	8.000	8.000	8.000	8.000	8.000	8.000
Al^{VI}	0.085	0.086	0.036	-	0.004	-	-	-
Ti	0.151	0.235	0.189	0.252	0.142	0.122	0.076	0.112
Fe^{3+VI}	0.831	0.303	0.396	0.537	0.338	0.141	0.841	0.633
Fe^{2+}	2.746	2.553	2.200	3.191	2.409	2.051	1.850	2.912
Mn	0.131	0.170	1.170	0.183	0.163	0.159	0.117	0.207
Mg	1.044	1.645	1.978	0.795	1.934	2.516	2.111	1.127
Zr	0.012	0.008	0.031	0.042	0.010	0.011	0.005	0.010
Σ	5.000	5.000	5.000	5.000	5.000	5.000	5.000	5.000
Ca_B	1.517	1.596	1.439	1.054	0.966	1.028	0.355	1.663
Na_B	0.483	0.404	0.561	0.946	1.034	0.972	1.645	0.337
Σ	2.000	2.000	2.000	2.000	2.000	2.000	2.000	2.000
Na_A	0.690	0.827	0.768	0.735	0.738	0.809	0.626	0.262
K_A	0.380	0.341	0.309	0.332	0.325	0.234	0.383	0.237
Σ	1.070	1.168	1.077	1.067	1.063	1.043	1.009	0.499
$Mg/Mg+Fe^{2+}$	0.27	0.39	0.47	0.20	0.45	0.55	0.53	0.28

*Fe_2O_3 determined after the method of Leake (1978)

1. Hastingsite, Mongolowe
2. Magnesian hastingsitic hornblende, Mongolowe
3. Ferro-edenitic hornblende, Chaone
4. Katophorite, Chinduzi
5. Katophorite, Chikala
6. Richterite, Mongolowe
7. Magnesio-arfvedsonite, Mongolowe
8. Ferro-edenite, Chikala

Analyses 1-7 are of amphiboles in foyaite and pulaskite; 8 is from a quartz syenite

Amphiboles. Selected amphibole analyses are presented in Table IV whereas the full compositional range has been plotted in the nomenclature diagrams of Leake, 1978 (fig. 5). The wide range of amphibole compositions is thus immediately apparent.

Amphiboles of the nepheline syenites fall into two distinct groups, the principal one (shaded in fig. 6) of which extends approximately from magnesian hastingsite to katophorite (fig. 5). This involves an increase in (Na+K), Si and Fe^{2+}, and a concomitant decrease in Ca and Mg (fig. 6*a* and *b*).

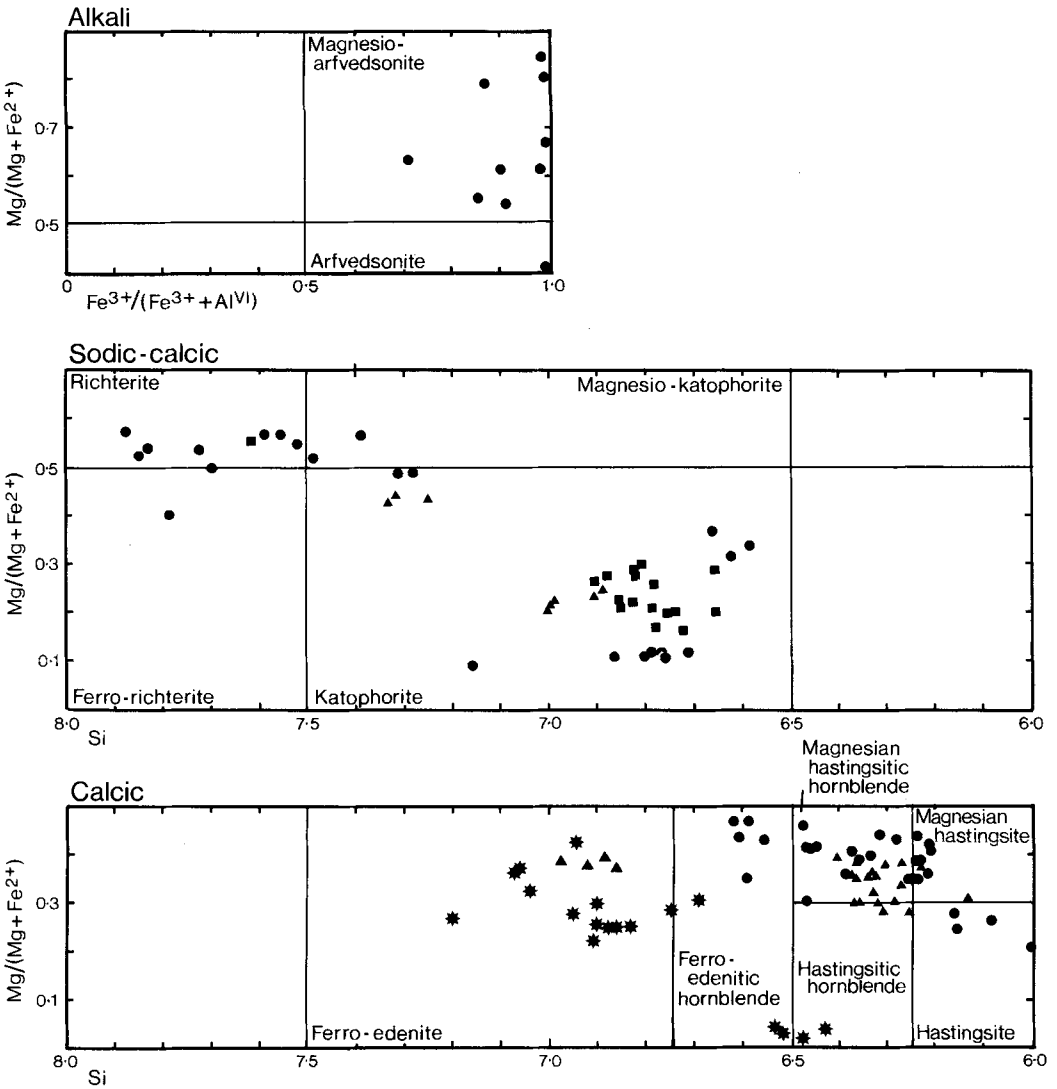

FIG. 5. Amphibole compositions plotted in terms of Si against $Mg/(Mg+Fe^{2+})$ and $Fe^{3+}/(Fe^{3+}+Al^{VI})$ against $Mg/(Mg+Fe^{2+})$. The compositional boundaries and amphibole nomenclature are based on Leake (1978). Circles, Mongolowe and Chaone; squares, Chinduzi; triangles, Chikala; stars, perthosites.

The Fe^{3+}/Fe^{2+} ratio may also increase but uncertainties inherent in the calculation of this ratio make this difficult to assess. The general increase in alkalinity and decrease in the Mg/Fe^{2+} ratio within this group broadly correlates with that shown by the pyroxenes, a phenomenon normal to both silica-undersaturated and oversaturated felsic alkaline rock series (Mitchell and Platt, 1978, 1982; Stephenson and Upton, 1982; Platt and Woolley, 1986).

These amphiboles occur as individual prisms or poikilitic crystals and are of primary igneous origin. Their compositional variation thus delineates a primary igneous evolution among the amphiboles.

The second group of amphiboles (outside the shaded area in fig. 6) in the nepheline syenites consists of lilac to blue richterite and magnesio-arfvedsonite (fig. 5). They display a reverse in the Mg/Fe^{2+} ratio of the igneous trend, having values typically greater than 0.45 (fig. 6*a*). Texturally, they

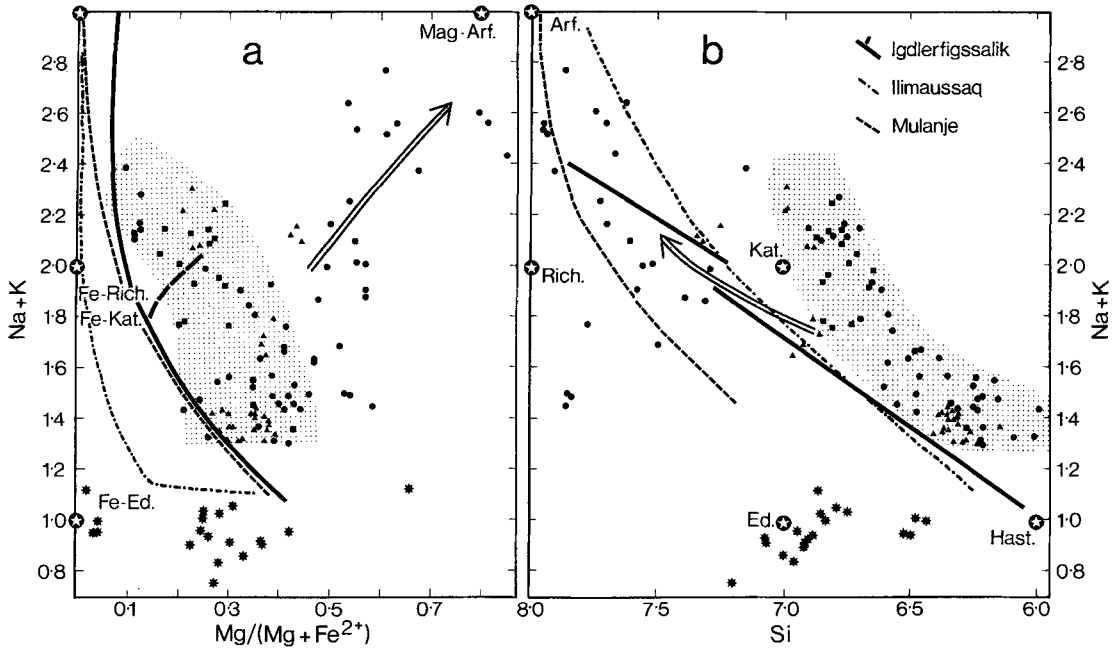

FIG. 6*a* and *b*. Plots of amphibole compositions in terms of (*a*) $Mg/(Mg+Fe^{2+})$ against (Na + K) and (*b*) Si against (Na + K). Symbols as in fig. 5. Stars in circles represent end-member compositions from Leake (1978). These are Mag-Arf, magnesio-arfvedsonite; Arf, arfvedsonite; Fe-Rich, ferro-richterite; Fe-Kat, ferri-katophorite; Rich, richterite; Kat, katophorite; Fe-Ed, ferro-edenite; Ed, edenite; Hast, hastingsite. The shaded areas are occupied by amphiboles of primary magmatic origin from nepheline syenites. Amphiboles of sub-solidus origin plot outside the shaded areas and the approximate trends defined are indicated by the double-shafted arrows. Stars are amphiboles from the perthosites. Trends for amphiboles from Ilimaussaq (Larsen, 1976), Igdlerfigssalik (Powell, 1978) and Mulanje (Platt and Woolley, 1986) are also shown.

are also distinctive, occurring as either late replacements of earlier amphiboles and pyroxenes or as narrow cross-cutting veinlets. Chemically, as well as texturally, they are very similar to the amphiboles of fenites and consequently a sub-solidus origin for them seems the most logical.

Trends of amphiboles from Ilimaussaq (Larsen, 1976) and Igdlerfigssalik (Powell, 1978) are given for comparison in fig. 6*a* and *b*. In terms of (Na + K) and Si (fig. 6*a*), the Malawi and Ilimaussaq trends are parallel but there is no apparent equivalent in Ilimaussaq of the Malawi sub-solidus series. Powell (1978), however, recognized a petrographically late, subsolidus blue amphibole from Igdlerfigssalik, here plotted as a subsidiary trend on fig. 6*a*. Extended amphibole series culminating in igneous arfvedsonites of low $Mg:Fe^{2+}$ ratio have been described from a number of oversaturated peralkaline complexes (Mitchell and Platt, 1978; Platt and Woolley, 1986). Such a trend for the Mulanje complex (Platt and Woolley, 1986) is also shown in fig. 6*a* and *b*.

In general, evolution towards alkali enrichment and lower $Mg:Fe^{2+}$ ratios occur in igneous amphiboles from both alkali-rich silica-undersaturated and oversaturated series. Higher Si values, however, appear to be characteristic of oversaturated series rocks which may reflect the higher Si activities of the magmas from which they form.

Igneous amphiboles from the silica-oversaturated perthosites have a substantially different trend of amphibole compositions (figs. 5 and 6*a* and *b*). Essentially ferro-edenitic in composition, there is little apparent variation in total alkalis but some in Si and Mg/Fe^{2+}. Whether this variation constitutes an evolutionary sequence is not clear from the available data, but these amphiboles are similar to the early crystallizing amphiboles of the Coldwell complex ferroaugite syenites (Mitchell and Platt, 1978). These were considered to have formed prior to the syenite magmas becoming alkali-enriched and peralkaline in character.

The marked differences between the perthosite

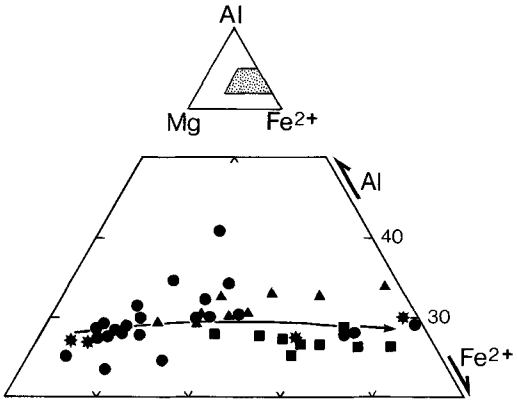

FIG. 7. Plot of biotites in terms of Al, Fe, and Mg. Symbols as in fig. 5.

amphiboles and those from the nepheline syenites substantiate the conclusion, based on petrochemistry (Woolley and Jones, in press) and pyroxene mineral chemistry (this paper), that the perthosites are not consanguineous with the nepheline syenites.

Biotite is a major phase in most of the nepheline syenites of Chaone, Mongolowe, and Chinduzi but is less common in those from Chikala. Selected analyses are given in Table V and the range of compositions in terms of Al, Mg, and total Fe, expressed as Fe^{2+}, is shown in fig. 7. The micas reported here are similar compositionally to those of Mulanje (Platt and Woolley, 1986) in which ferric iron was minimal. Consequently, reporting total iron in the ferrous form seems reasonable.

Essentially constant in Al content, the biotites show variations in Fe^{2+} : Mg ratios from 0.50 to 0.99, the latter being essentially annites. The observed compositional range is similar for each of the complexes although the biotites from Mongolowe and Chaone are dominated by more Mg-rich compositions (fig. 7). Those from Chikala and Chinduzi are generally richer in iron and it is from these complexes that the bulk of the annites have been analysed.

Similar trends to those reported here have been observed in such complexes as Shonkin Sag (Nash and Wilkinson, 1970), Kungnat Fjeld (Stephenson and Upton, 1982), and Mulanje (Platt and Woolley, 1986).

Micas of the perthosites, although only limited

TABLE V

REPRESENTATIVE ANALYSES OF MICAS

	1	2	3	4	5	6
SiO_2	33.99	35.56	37.97	35.37	36.22	36.07
TiO_2	5.29	4.65	2.86	3.81	2.95	3.17
Al_2O_3	10.65	13.02	11.91	10.31	11.78	12.53
FeO*	36.26	22.61	21.19	33.43	26.10	26.64
MnO	0.97	0.84	0.99	1.26	0.96	0.90
MgO	0.28	9.93	12.00	3.75	9.01	7.57
CaO	0.00	0.05	0.00	0.02	0.05	0.00
Na O	0.62	0.59	0.77	0.66	0.68	0.22
K O	9.19	9.87	10.06	9.29	9.89	10.04
ZrO	-	0.08	0.11	0.17	0.11	0.00
Total	97.25	97.20	97.86	98.07	97.75	97.14
	Structural formula based on 22 oxygens					
Si	5.631	5.497	5.765	5.726	5.971	5.668
Ti	0.659	0.541	0.327	0.464	0.366	0.375
Al	2.080	2.372	2.131	1.967	2.289	2.321
Fe*	5.024	2.923	2.691	4.526	3.598	3.501
Mn	0.136	0.110	0.127	0.173	0.134	0.120
Mg	0.069	2.264	2.715	0.905	0.985	1.773
Ca	0.000	0.008	0.000	0.003	0.009	0.000
Na	0.199	0.177	0.227	0.207	0.217	0.067
K	1.942	1.946	1.949	1.919	2.080	2.013
$\frac{Fe^{2+}+Mn}{Fe^{2+}+Mn+Mg}$	0.99	0.57	0.51	0.84	0.79	0.67

*Total iron as FeO

1-2 Mongolowe; 3 Chaone; 4 Chinduzi; 5-6 Chikala

compositional data are available, appear to mimic the overall trend of the nepheline syenites. On this basis at least, the perthosites cannot be differentiated from the nepheline syenites.

Minor phases. Typical accessory minerals in all the nepheline syenites are apatite, sphene, and zircon. The comparatively rare minerals catapleiite, rosenbuschite and låvenite occur as very minor late-stage phases in the Chinduzi rocks: låvenite has also been found in Chikala, as has zirconolite. None of these phases, as far as is known, occurs in the nepheline syenites of Chaone and Mongolowe. Analyses of some of these uncommon minerals are given in Table VI.

TABLE VI

ANALYSES OF LAVENITE, ROSENBUSCHITE AND CATAPLEIITE FROM CHINDUZI

	Lavenite		Rosenbuschite		Catapleiite
SiO_2	28.64	28.71	29.64	30.21	47.37
TiO_2	2.51	5.05	6.22	6.62	0.00
Al_2O_3	0.00	0.00	0.00	0.12	0.00
FeO*	5.36	7.01	1.07	1.24	0.56
MnO	2.79	3.43	1.39	1.41	0.00
MgO	0.04	0.02	0.05	0.08	0.00
CaO	9.64	11.07	23.08	23.20	1.42
Na_2O	11.93	11.18	10.01	9.79	7.72
K_2O	0.00	0.06	0.09	0.00	0.00
ZrO_2	28.47	22.87	17.76	17.46	34.18
Nb_2O_5	5.18	3.90	0.40	0.70	NA
Total	94.56	93.30	89.71	90.83	91.25

*Total iron as FeO

Chevkinite has been identified in a quartz syenite from Chikala and this mineral, together with zirconolite, is discussed in a forthcoming paper (Platt *et al.*, in press) and will not be further elaborated on here.

Discussion

The close spatial relationship of the four nepheline syenite complexes of Chikala, Chaone, Mongolowe, and Chinduzi and their essential geochemical coherence (Woolley and Jones, in press) strongly suggests some fundamental relationship in their formation. This is in part supported by the limited age data from Chaone (138 ± 14 Ma; Bloomfield, 1961) and Chinduzi (116 ± 6 Ma; Cahen and Snelling, 1966). It would seem unreasonable, therefore, to infer that the individual complexes were the product of unrelated magmas. Rather, it is more reasonable to propose a fundamental relationship between the magmas forming the various complexes.

Clues to this relationship are manifest in the pyroxene data obtained from each of the four complexes. Taken individually, each appears to have developed from broadly similar magmas under different conditions of oxidation potential and perhaps even alkali activity. This would account for the different paths of alkali enrichment in the pyroxenes when expressed in terms of acmite, diopside, and hedenbergite (figs. 3*a–d* and 4). Essentially, crystallization under conditions producing low-magmatic Fe^{2+}/Fe^{3+} ratios, i.e. enhanced oxidation potential (Nash and Wilkinson, 1970; Stephenson and Upton, 1982; Platt and Woolley, 1986) and/or alkali activity (Fudali, 1965; Paul and Douglas, 1965), enhances the formation of acmite-enriched pyroxenes. With the reverse situation, pyroxenes in felsic alkaline rocks tend to become enriched in hedenbergite. These general principles hold true irrespective of the silica activity of such magmas (cf. Nash and Wilkinson, 1970; Larsen, 1976; Mitchell and Platt, 1978 and 1982; Platt and Woolley, 1986).

The individual pyroxene trends of the nepheline syenite complexes (fig. 4) indicate that acmite enrichment occurs somewhat earlier in the pyroxenes of Mongolowe and Chaone than in those of Chikala and Chinduzi. In consequence, the aegirine-augites of Mongolowe and Chaone are somewhat more enriched in Mg. The relative roles of oxidation potential and alkali activity in determining the various trends are difficult to assess although, as indicated previously, the more peralkaline nature of Chinduzi suggests that, in this complex at least, the effects of alkali activity may have been significant.

If the salitic pyroxenes of the individual trends are considered as a group, they form a single trend becoming enriched in hedenbergite (fig. 4). From this 'salitic trend', indicated by the shaded arrow on fig. 4, the individual trends of acmite enrichment are seen to branch at points of increasing hedenbergite enrichment. Viewed from this perspective, it is advisable to consider the individual pyroxene trends as forming from two discrete stages of development: an earlier or fundamental stage, the conditions of which controlled salite development and a more advanced stage, the conditions of which controlled acmite enrichment of the later pyroxenes.

The two-stage development of early salitic pyroxenes and later sodium-enriched pyroxenes may well reflect a two-stage history of magmatic development. A reasonable model for this would have (1) a fundamental stage in which a source magma was pooled at depth and (2) a complex-

forming stage in which the source magma was periodically injected into shallow chambers to form the individual nepheline syenite complexes. Evidence to support shallow level emplacement includes the presence of xenoliths and down-faulted blocks of Chilwa volcanics, cauldron subsidence and, as discussed previously, the presence of relatively high-temperature nephelines.

Such a two-stage model is attractive as it accounts for a number of features observed in the field. Periodic tapping of the source magma would account for the multiple intrusive character of the individual complexes. Moreover, migration of emplacement with time, perhaps in conjunction with associated volcanic activity, would also account for the overlapping of individual complexes.

Mineralogically, the salitic trend of the pyroxenes is equated with the fundamental stage and evolution of the source magma at depth, whereas later sodium enrichment is thought to have occurred after magmatic emplacement at shallow levels. On the basis of salite and aegirine-augite compositions, as discussed previously, the two-stage model would suggest that the magmas of Mongolowe and Chaone migrated to their higher-level chambers somewhat earlier than those of Chikala, with those from Chinduzi migrating somewhat later still. The more peralkaline nature of the Chinduzi magmas may be a response to a greater degree of evolution of the source magma before emplacement. Extending this argument to the Junguni complex, the most peralkaline of all the nepheline syenites, lying just to the north of the main group (fig. 1), this may form from an even more evolved version of the source magma.

The mineral chemistry of the amphiboles and micas broadly correlates with that of the pyroxenes in that magnesio-hastingsitic hornblende (fig. 5) and the more magnesian biotites (fig. 7) occur with the more diopside-rich pyroxenes of Chaone and Mongolowe, whereas katophorites and annites are characteristically associated with the pyroxenes of the more peralkaline complex of Chinduzi (fig. 4). Petrographic evidence suggests that both hydrous phases crystallized later than the salitic pyroxenes, presumably under the conditions then operative within the individual high-level magma chambers.

The general trends of amphibole and biotite evolution (figs. 6*a* and *b*, and 7) should be considered therefore as composite trends reflecting conditions of crystallization within the high-level chamber of each of the complexes. However, in so far as the parental magmas of each of these complexes are thought to reflect the evolution of a fundamental magma at depth, some control of the subsequent amphibole and mica evolution must originate with the nature of the fundamental magma at the time of high-level emplacement. The close association of magnesian hastingsitic amphiboles and magnesian biotites with the more diopsidic salites, and katophorites and annites with more hedenbergitic salites provides evidence for this.

The nature of the fundamental magma and the conditions under which it crystallized are difficult to assess. That it was felsic and silica-undersaturated would seem reasonable in the light of the total lack of gabbroic rocks associated with any of the complexes and their obvious silica-undersaturated character. Evolution of salitic pyroxenes towards more hedenbergite-rich compositions within the magma suggests crystallization under relatively low oxidation potentials and the lack of early crystallizing amphiboles indicates crystallization under comparatively low partial pressures of water. Unfortunately, estimates of such intensive parameters as oxygen fugacity, silica activity and crystallization temperatures cannot be defined by the present data.

On the basis of nepheline compositions, it is reasonable to predict crystallization temperatures within the high-level chambers of between 950 and 750 °C. Subsequently, rather rapid cooling prevented re-equilibration to the Morozewicz–Buerger convergence field. Oxygen fugacities prevailing are difficult to estimate although the presence of biotite/annite, alkali feldspar and magnetite in each of the complexes gives some indication (Nash and Wilkinson, 1970). At constant temperature, increasing annite content of the mica occurs as a function of falling f_{O_2} whereas with falling temperature at constant f_{O_2} the molecular fraction of annite in biotite decreases (op. cit., fig. 8). In each of the complexes, biotite evolution is one of increasing annite content indicating a decrease in f_{O_2} with falling temperature. Micas from Mongolowe show the most extensive variation in composition with $(Fe^{2+}+Mn)/(Fe^{2+}+Mn+Mg)$ ratios of between 0.51 and 0.99. For the crystallization temperatures indicated above, this corresponds with an approximate range of f_{O_2} between 10^{-15} bars (950 °C) and 10^{-19} bars (750 °C). This corresponds well with f_{O_2} from the broadly similar nepheline syenites of the Coldwell complex which were estimated to be 10^{-14} to 10^{-19} bars for a temperature range of 900 to 700 °C (Mitchell and Platt, 1982). A similar range of mica compositions is observed in the rocks of Chaone, but the ranges for Chikala and Chinduzi are more restricted, with $(Fe^{2+}+Mn)/(Fe^{2+}+Mn+Mg)$ values of 0.66–0.98 for the former and 0.69–0.94 for the latter. This could indicate either a lower f_{O_2} (i.e. 10^{-17} bars) for these magmas at 950 °C when compared with those

of Chaone/Mongolowe or lower temperatures of initial mica crystallization, but it is impossible to discriminate between these two alternatives. At 750 °C, however, the magmas of all the complexes appear to have very similar f_{O_2} (i.e. approximately 10^{-19} bars).

Subsolidus crystallization in the nepheline syenites generated small amounts of aegirine, richterite, and magnesio-arfvedsonite in rocks of Mongolowe and Chaone (figs. 3*a* and *b*, and 6*a* and *b*). The amphiboles, in particular, show a reverse in the general iron-enrichment trend of the igneous amphiboles (fig. 6*b*). In this respect, this late crystallization is remarkably similar to fenites in which iron-rich sodic pyroxenes coexist with magnesium-rich amphiboles (Vartiainen and Woolley, 1976, fig. 38). It is not clear whether Mg needs to be introduced into the rocks containing the magnesio-arfvedsonites and richterites, or whether dissolution of earlier pyroxenes and amphiboles is the Mg source. The rather variable (Na+K) and Mg/(Mg+Fe^{2+}) ratios of the late amphiboles (fig. 6*a*) probably reflects the heterogeneities to be expected in relatively open subsolidus systems.

Although not the major subject of this paper, the silica-oversaturated perthosites spatially associated with the nepheline syenites—and therefore possibly genetically associated with these undersaturated magmas—seem, from the limited mineralogical data, to be, in fact, unrelated. In particular, the salitic pyroxene trend (figs. 3*d* and 4) is substantially different, evolving as it does to compositions extremely rich in hedenbergite. Moreover, Na enrichment is not observed in the perthosite pyroxenes. This trend is similar to that seen in the early stages of pyroxene evolution of the quartz syenites from Mulanje (Platt and Woolley, 1986) and Zomba (Woolley and Jones, in prep.). Similarly, the amphiboles in the perthosites are quite different from those of the nepheline syenites (figs. 5 and 6). Rather than being related to the nepheline syenite magmatism, it is concluded that the perthosites are related to a silica-oversaturated alkali magmatism and, logically, this would be associated with the development of the Zomba complex situated a few kilometres to the south (fig. 1).

Acknowledgements. The authors would like to express their appreciation to the Government of Malawi for permission to undertake the field work. We are most grateful to Drs A. C. Bishop, D. R. C. Kempe and R. H. Mitchell for critically reading the manuscript, and to Miss V. Jones for drafting the figures. We thank Miss F. Wall and Mr G. C. Jones for technical assistance with the microprobe work. R.G.P. also acknowledges support for the project from NSERC operating grant A9169.

REFERENCES

Bloomfield, K. (1961) The age of the Chilwa Alkaline Province. *Rec. Geol. Surv. of Malawi* **1,** 95–100.

——(1965) The geology of the Zomba area. *Bull. Geol. Surv. of Malawi* **16,** 193 pp.

Cahen, L., and Snelling, N. J. (1966) *The geology of equatorial Africa.* North-Holland Publishing Company, Amsterdam. 195 pp.

Fudali, R. F. (1965) Oxygen fugacities of basaltic and andesitic magmas. *Geochim. Cosmochim. Acta,* **29,** 1063–75.

Garson, M. S. (1960) The geology of the Lake Chilwa area. *Bull. Geol. Surv. of Nyasaland,* **12,** 67 pp.

——(1962) The Tundulu carbonatite ring-complex in southern Nyasaland. *Mem. Geol. Surv. of Nyasaland,* **2,** 248 pp.

—— and Smith, W. Campbell (1958) Chilwa Island. Ibid. **1,** 127 pp.

Hamilton, D. L. (1961) Nephelines as crystallization temperature indicators. *J. Geol.* **69,** 321–9.

Larsen, L. M. (1976) Clinopyroxenes and coexisting mafic minerals from the alkaline Ilimaussaq intrusion, South Greenland. *J. Petrol.* **17,** 258–90.

Leake, B. E. (1978) Nomenclature of amphiboles. *Mineral. Mag.* **42,** 533–63.

Mitchell, R. H., and Platt, R. G. (1978) Mafic mineralogy of ferroaugite syenite from the Coldwell alkaline complex, Ontario, Canada. *J. Petrol.* **19,** 627–51.

——(1982) Mineralogy and petrology of nepheline syenites from the Coldwell alkaline complex, Ontario, Canada. Ibid. **23,** 186–214.

Nash, W. P., and Wilkinson, J. F. G. (1970) Shonkin Sag laccolith, Montana. I. Mafic minerals and estimates of temperature, pressure, oxygen fugacity and silica activity. *Contrib. Mineral. Petrol.* **25,** 241–69.

Paul, A., and Douglas, R. W. (1965) Ferrous-ferric equilibrium in binary alkali silicate glasses. *Phys. Chem. Glasses* **6,** 207–11.

Platt, R. G., and Woolley, A. R. (1986) The mafic mineralogy of the peralkaline syenites and granites of the Mulanje complex, Malawi. *Mineral. Mag.* **50,** 85–99.

——Wall, F., Williams, C. T., and Woolley, A. R. (in press) Zirconolite, chevkinite and other rare earth minerals from nepheline syenites and peralkaline granites and syenites of the Chilwa Alkaline Province, Malawi. *Mineral Mag.* **51.**

Powell, M. (1978) The crystallisation history of the Igdlerfigssalik nepheline syenite intrusion, Greenland. *Lithos,* **11,** 99–120.

Stephenson, D., and Upton, B. G. J. (1982) Ferromagnesian silicates in a differentiated alkaline complex: Kungnat Fjeld, South Greenland. *Mineral Mag.* **46,** 283–300.

Stillman, C. J., and Cox, K. G. (1960) The Chikala Hill syenite-complex of southern Nyasaland. *Trans. Proc. Geol. Soc. S. Afr.* **63,** 99–117.

Tilley, C. E. (1954) Nepheline-alkali feldspar paragenesis. *Am. J. Sci.* **252,** 65–75.

Vail, J. R., and Mallick, D. I. J. (1965) The Mongolowe Hills nepheline-syenite ring-complex, southern Malawi. *Geol. Surv. Malawi Rec.* **3,** 49–60.

Vail, J. R., and Monkman, L. J. (1960) A geological reconnaissance survey of the Chaone Hill ring complex, southern Nyasaland. *Trans. Proc. Geol. Soc. S. Afr.* **63,** 119–35.

Vartiainen, H., and Woolley, A. R. (1976) The petrography, mineralogy and chemistry of the fenites of the Sokli carbonatite intrusion, Finland. *Bull. Geol. Surv. Finland.* **280,** 1–87.

Woolley, A. R., and Garson, M. S. (1970) Petrochemical and tectonic relationship of the Malawi carbonatite-alkaline province and the Lupata-Lebombo volcanics. In *African magmatism and tectonics* (T. N. Clifford and I. G. Gass, eds.). Oliver and Boyd, Edinburgh. 237–62.

——and Jones, G. C. (in press) The petrochemistry of the northern part of the Chilwa Alkaline Province, Malawi. *Geol. Soc. London Spec. Publ.*

[*Manuscript received 10 January 1986; revised 10 February 1986*]